Neoplasma 2022; 69(6): 1359–1372

doi:10.4149/neo_2022_220727N774

miR-550a-5p promotes the proliferation and migration of hepatocellular carcinoma by targeting GNE via the Wnt/β-catenin signaling pathway

Chun-Ming LI[1,#], Wu WU[1,#], Zhu ZHU[1], Pei-Lin LU[2], Jian-Ping GONG[1], Rong MA[1,*]

[1]Department of Hepatobiliary Surgery, The Second Affiliated Hospital of Chongqing Medical University, Chongqing, China; [2]Department of Dermatology, The First Affiliated Hospital of Chongqing Medical University, Chongqing, China

**Correspondence: marong@hospital.cqmu.edu.cn*
#Contributed equally to this work.

Received July 27, 2022 / Accepted October 28, 2022

Liver cancer is one of the most common tumors with a high malignant degree in the world. Its diagnosis and treatment are very difficult and limited. More novel and powerful DAT strategies are urgently needed to break this situation. An increasing number of studies have shown that microRNAs (miRNAs) could be used not only as biomarkers for the diagnosis and prognosis of hepatocellular carcinoma (HCC) but also as important targets for molecular targeted therapy. However, the role of miR-550a-5p in HCC and its specific mechanism remain unclear. Here we proposed and verified the hypothesis that the miR-550a-5p could regulate the progression of HCC and was positively associated with poor prognosis. We found that decreased miR-550a-5p would inhibit the proliferation and migration of HCC cell lines (HCs) by performing relevant assays. Interestingly, knocking down GNE could reverse the above effect of miR-550a-5p on HCs. Meanwhile, the western blot results showed that the Wnt/β-catenin signaling pathway was at least partly involved in the regulation of HCC by miR-550a-5p. In addition, we also found that miR-550a-5p could suppress the growth of HCC *in vivo* via a xenograft tumor model assay. All in all, we draw a conclusion that the miR-550a-5p/GNE axis functioned as an important role in promoting the progression of HCC via the Wnt/β-catenin signaling pathway.

Key words: miR-550a-5p, GNE, Wnt/β-catenin; HCC

Hepatocellular carcinoma (HCC) is currently the second leading cause of cancer-related death [1]. At present, the occurrence of HCC is related to some chemical carcinogens (viral hepatitis, cirrhosis, aflatoxin, water and soil pollution, etc.), but the specific mechanism is still unclear accompanied by the difficult diagnosis and treatment (DAT). Moreover, early-stage HCC lacks typical clinical manifestations. Although relevant imaging examinations (ultrasound, CT, MRI, etc.) and alpha-fetoprotein (AFP) detection are helpful for early diagnosis, the sensitivity is still limited. Currently, surgical resection is still the main treatment for HCC, but only ~30% of HCC patients can undergo an operation when the diagnosis is confirmed [2]. Therefore, it is of great significance to elucidate the specific underlying molecular mechanism of HCC to improve the DAT efficiency.

miRNAs are endogenous noncoding small interfering RNAs composed of ~21–25 nucleotides [3]. miRNAs negatively regulate the expression of target genes by binding to the 3'-untranslated region (UTR) of mRNA [4]. The biological processes of miRNAs include transcription, cleavage, output, further cleavage, chain selection, binding and interaction with mRNA [5, 6]. miRNAs have been reported to regulate the expression of approximately 30% of human genes, many of which are involved in the development and progression of tumors [7]. Some studies confirmed that miRNAs were closely related to the occurrence and development of HCC, and identified that miRNAs could function as biomarkers to play significant roles in the DAT of HCC [8, 9]. However, the role of miR-550a-5p in HCC and its specific mechanism are still vague.

Glucosamine UDP-N-acetyl-2-epimerase/N-acetylmannosamine kinase (GNE), a bifunctional enzyme that initiates and regulates the biosynthesis of N-acetylneuraminic acid (NeuAc), is a precursor of sialic acids [10]. Mutations of GNE are associated with autosomal recessive [11] inclusion body myopathy [12] and Nonaka myopathy [13] by sialic acid modification of cell surface molecules. Sialic acids can also regulate multiple biological processes, such as cell adhesion and signal transduction, to take part in the tumorigenicity and metastatic behavior of malignant cells [14,

15]. A recent study defined GNE as a significant biomarker related to the prognosis of HCC using long noncoding RNA (lncRNA)-associated competing endogenous RNA (ceRNA) analysis [16]. However, the precise mechanism of GNE in HCC remains unknown. The Wnt/β-catenin signaling pathway plays an important role in the development of HCC. Currently, the Wnt/β-catenin signaling pathway has three main branches: the classic Wnt/β-catenin signaling pathway, the Wnt/planar cell polarity (PCP) pathway, and the Wnt/Ca^{2+} pathway [17]. β-catenin, as the most important biomarker in the classical Wnt pathway, inhibits its degradation by reducing the phosphorylation of upstream protein kinases during Wnt signal activation and then enters the nucleus and binds to the TCF/LEF transcription factor family to initiate transcription of downstream target genes [18, 19].

In this study, we linked the above three targets in series and reported that the miR-550a-5p/GNE/Wnt/β-catenin axis was involved in the modulation of the malignant progression of HCC for the first time.

Patients and methods

Bioinformatic analysis. All the RNA expression profiles and clinical data of HCC in this work were downloaded from TCGA online database (https://portal.gdc.cancer.gov/). RStudio was applied to screen the differentially expressed miRNAs (DEms) and draw relevant visualization pictures including heatmap, volcano map, survival analysis curve, etc. R packages involved in the above work were "Limma", "edgeR", "DEseq2", "ggplot2", etc. Target genes of miR-550a-5p were predicted by miRDB (http:// mirdb.org/) and Target Scan (http://www.targetscan.org/vert_72/). Venny2.1.0 (https://bioinfogp.cnb.csic.es/tools/venny/index.html) was used to show the potential candidate target genes of miR-550a-5p by taking the intersection.

Patients and tissue samples. In this study, mRNA, miRNA, and protein were detected in tumor tissues (T) and paired paracancer normal tissues (N) of 10 pathologically diagnosed HCC patients hospitalized at the Department of Hepatobiliary Surgery, the Second Affiliated Hospital of Chongqing Medical University between May 2011 and July 2012. Before collecting patient samples, we informed patients and their families and signed informed consent for clinical sample collection. This study was approved by the Ethics Committee of the Second Affiliated Hospital of Chongqing Medical University and was in accordance with the Declaration of Helsinki.

Table 1. The primer sequences for qRT-PCR.

Primer name	Prime direction	Primer sequence (5'–3')
miR-550a-5p	Forward	TGCTGTTAGGTTGTCTTCA
	Reverse	CTATGTTTTGTCCAATTTCT
U6	Forward	CTCGCTTCGGCAGCACATATACT
	Reverse	ACGCTTCACGAATTTGCGTGTC
GNE	Forward	GACTTTGACATTAACACCAGGCT
	Reverse	GCTTCAGGCGATTAAGGACATCT
β-actin	Forward	CCTTCCTGGGCATGGAGTCCT
	Reverse	GGAGCAATGATCTTGATCTT

Cell culture and transfection. HCs (LM3, HepG2, and Huh7) and the normal liver cell line LO2 were all obtained from the Institute of Biochemistry and Cell Biology (Chinese Academy of Sciences, Shanghai, China). All the cell lines were cultured in Dulbecco's modified Eagle's medium (Gibco, USA) containing 10% fetal bovine serum (FBS, Gibco, USA) and 100 U/ml penicillin and streptomycin (HyClone, USA) in a humidified incubator with 5% CO_2 at 37 °C. Cells were transfected with related plasmids using Lipofectamine 2000 (Invitrogen) based on the manufacturer's instructions. The miR-550a-5p inhibitor (5'-GGGCUCUUACUCCCUCAGGCACU-3'), GNE siRNA (5'-GUACCCUUGUUCAAAGAUAUA-3'), and their associated controls were obtained from GenePharma (Shanghai, China).

Quantitative real-time PCR (qRT-PCR). TRIzol Reagent (Invitrogen, 15596018) was used to extract total RNA from tissues or cells according to a previously described protocol [20]. Genomic DNA was removed from the RNA and reversely transcribed into cDNA using the PrimeScript RT Reagent kit (TaKaRa). The expression level of RNA was measured by qRT-PCR with TB Green Premix Ex Taq II (TaKaRa). U6 was used as the internal reference for miRNA, while β-actin was used as the internal control for mRNA. The primer sequences involved in this experiment are shown in Table 1.

Cell-counting kit-8 assay. The cell-counting kit-8 assay (CCK-8, Bimake, USA) was used to analyze the proliferation according to the manufacturer's instructions. Huh7 and LM3 cells were seeded in 96-well plates at 3,000 cells/well. At 24, 48, and 72 h respectively after transfection, 10 μl CCK-8 reagent was added to each well and incubated at 37 °C for 2 h. Then, the absorbance at 450 nm was detected to assess the proliferation for each well.

5-ethynyl-2'-deoxyuridine (EdU) assay. The 5-ethynyl-2'-deoxyuridine (EdU) (Beyotime, China) assay was used to assess cell proliferation according to the manufacturer's instructions. Briefly, 5×10^4 Huh7 and LM3 cells were cultured in 24-well plates. After 24 h, the cells were incubated with preheated EdU (10 μM) for 2 h at 37 °C and fixed in 4% formaldehyde for 15 min. After washing with phosphate-buffered saline (PBS) 3 times, 0.3% Triton X-100 solution was used to permeabilize the cells for 10 min at room temperature. After washing again, the click additive solution proceeded for 30 min in the dark room. To measure the percentage of cell proliferation, cells were stained by adding 1× Hoechst 33342 for 10 min at room temperature in the dark. Typical images were photographed under an inverted microscope, and the rate of EdU-positive cells was measured by ImageJ.

Colony formation assay. Huh7 and LM3 cells were plated in 6-well plates (500 cells/well) containing 2 ml of culture

medium and cultured for 2–3 weeks to form colonies. Colonies were fixed in 4% formaldehyde for 15 min and stained with 0.1% crystal violet for 30 min. The colonies were counted to assess cell proliferation.

Wound healing assay. Briefly, 5×10^5 Huh7 and LM3 cells were grown in 6-well plates until complete confluence. After washing with PBS, a 200 μl pipette tip was used to scratch the cells. After 0, 24, and 48 h, the cells were photographed under an inverted microscope, and the area of the wound was measured by ImageJ.

Transwell assay. Transwell assays were performed to assess cell migration using 24-well Transwell chambers. The lower chamber was filled with 500 μl DMEM containing 10% FBS, while 100 μl DMEM containing a cell suspension was added to the upper chamber at a density of 1×10^5 cells/ml. After 24 h, the Transwell chambers were removed, fixed in 4% formaldehyde for 15 min, and stained with 0.1% crystal violet for 10 min. The cells were counted and photographed under an inverted microscope.

Mouse xenograft tumor model. 6-week-old male BALB/c-nu mice were purchased from GemPharmatech Co., Ltd. (Chengdu, China) and fed in the Experimental Animal Center of Chongqing Medical University (Chongqing, China). The mice were cared for in accordance with the Regulations for the Administration of Affairs Concerning Experimental Animals. Anti-miR-550a-5p and its associated negative control Huh7 and LM3 cells (5×10^6) were subcutaneously injected into the right axillary side of the mice to assess cell proliferation *in vivo*. Tumor volume was calculated by the formula: volume = (width^2 × length)/2. Tumor volume was measured every three days after being visible to the naked eye. At 17 days after injection, the mice were sacrificed, and tumors were collected for further experiments.

Western blot. The total proteins of tissues or cells were extracted using RIPA lysis buffer (Beyotime, China). The samples were incubated on ice for 15 min, and the supernatant was collected after 12,000 × g at 4 °C for 10 min. A bicinchoninic acid kit (Beyotime, China) was used to determine the protein concentration according to the manufacturer's instructions. After adding the loading buffer (Beyotime, China), the proteins were separated by sodium dodecyl sulfate-polyacrylamide gel electrophoresis and transferred to a nitrocellulose transfer membrane (GE Healthcare, USA). The membranes were blocked with 5% nonfat powdered milk at room temperature for 1 h, and the blots were probed overnight at 4 °C with the following specific primary antibodies: GNE (Proteintech, 25079-1-AP, 1:1000), GAPDH (Proteintech, 10494-1-Ig, 1:5000), Ki-67 (CST, 9449, 1:1000), Vimentin (CST, 3932, 1:1000), N-Cadherin (CST, 14215, 1:1000), E-Cadherin (CST, 14472, 1:1000), c-Myc (CST, 13987, 1:1000), β-Catenin (CST, 8480, 1:1000), MMP2 (Proteintech, 10373-2-AP, 1:1000), and MMP9 (Proteintech, 10375-2-AP, 1:1000). After washing 3 times with Tris-buffered saline Tween-20 (TBST), the membrane was incubated with anti-rabbit immunoglobulin G (IgG) (CST, 7074, 1:5000) or anti-mouse immunoglobulin G (IgG) (CST, 7076, 1:5000) secondary antibody at room temperature for 1 h. After washing, the protein bands were visualized using a Bio-Rad Image Analysis System (BIO-RAD, USA) with an enhanced chemiluminescence Fluorescence Detection kit (GE HealthCare, USA). WB experiment was performed three times independently and the quantification of WB band intensities was measured by ImageJ.

Immunohistochemistry. Paraffin-embedded tumor tissues from mice were cut into 3 μm slices. Sodium citrate solution (Beyotime, China) was used for antigen repair, and immunohistochemistry (IHC) was performed using a polymer horseradish peroxidase detection system (Zhongshan Goldenbridge Biotechnology, China). The sections were incubated with the following specific primary antibodies: Ki-67 (CST, 9449, 1:800) and Cyclin B2 (Proteintech, 21644-1-AP, 1:200). Typical images were photographed under the inverted microscope, and positive areas of the staining were counted by ImageJ.

Luciferase reporter assay. The plasmids containing the 3'-UTR sequence or the mutant sequence of GNE were designed by Genechem (Shanghai, China). LM3 cells were cultured in 24-well plates transfected with miR-550a-5p mimics or its associated control (control) and WT or MUT luciferase reporter plasmids. 48 h later, the cells were collected, and luciferase assays were performed using a Dual-Luciferase Assay Kit (Promega) according to the manufacturer's instructions.

Statistical analysis. GraphPad Prism Version 6.0 (CA, USA) and SPSS 25 Software (SPSS Inc., USA) were used to analyze the data. The measurement data are expressed as the mean ± standard deviation (SD). The t-test was performed for comparisons between two groups, while one-way analysis of variance (ANOVA) was used for comparisons among multiple groups. The Kaplan-Meier method was used for the survival analysis. A p-value <0.05 indicated statistical significance.

Results

miR-550a-5p was highly expressed in HCC patients and was positively associated with poor prognosis. To explore new treatment strategies, we downloaded and analyzed the miRNA data of HCC from TCGA online website. The results demonstrated that miR-550a-5p was one of the top 30 upregulated miRNAs in HCC samples compared with that in normal samples (Figures 1A–1C). In addition, the survival analysis results showed that patients with higher expression levels of miR-550a-5p had lower survival rates, indicating that miR-550a-5p exerted a significant effect on the survival of HCC patients (Figure 1D). Subsequently, qPCR was applied to verify the expression level of miR-550a-5p in 10 pairs of liver cancer tissues and their adjacent tissues, and the results demonstrated that miR-550a-5p was highly expressed in tumor tissues from our center (Figure 1E).

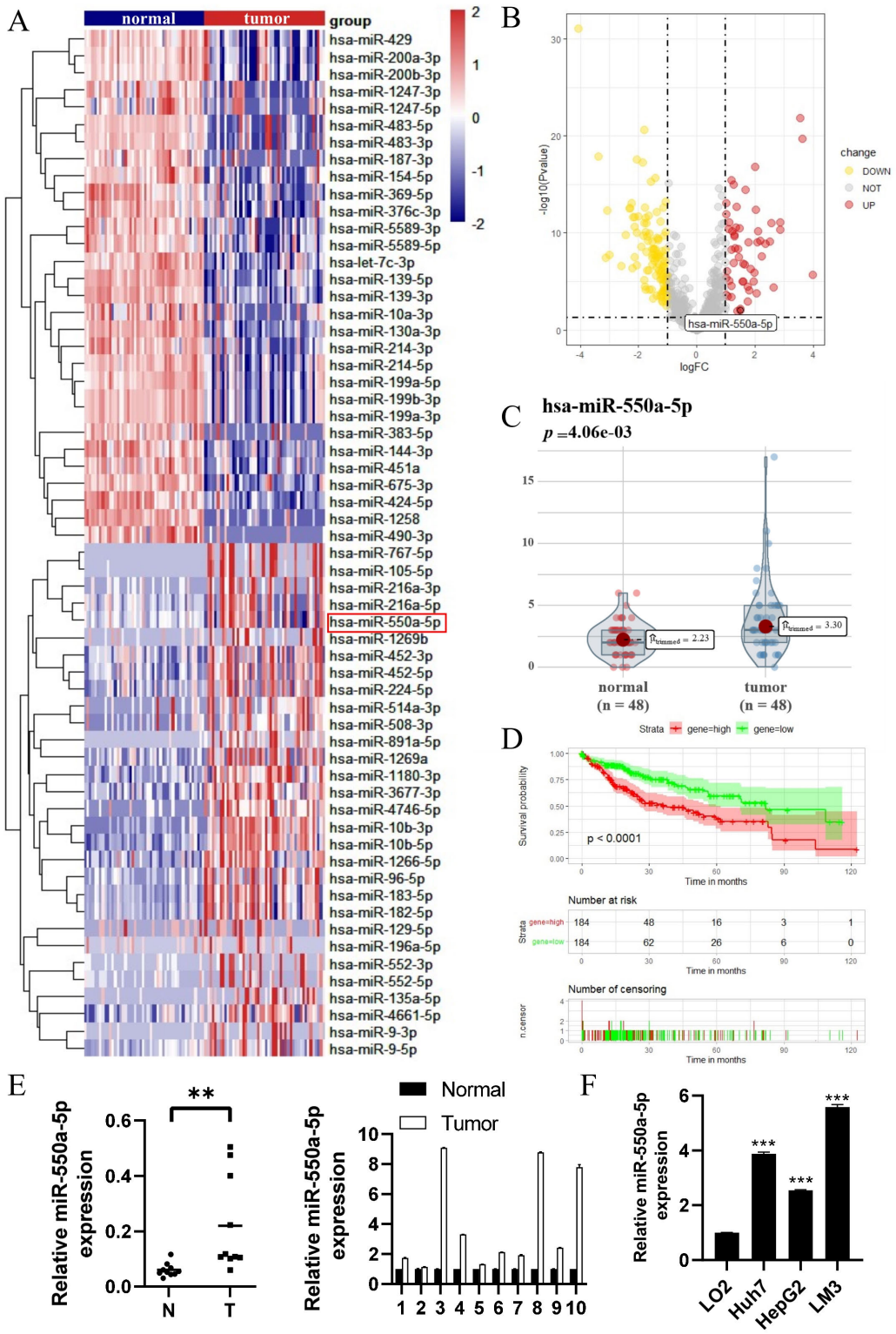

Figure 1. miR-550a-5p is highly expressed in hepatocellular carcinoma (HCC) patients and HCC cell lines (HCs). The heatmap (A) and the volcano map (B) of the top 30 differentially expressed miRNAs for HCC samples from TCGA database. The miR-550a-5p was highlighted. C) Relative expression of miR-550a-5p in 48 pairs of HCC samples from TCGA database. D) Kaplan-Meier analysis of overall survival between high (n=184) and low (n=184) miR-550a-5p expression in HCC patients. E) Relative expression of miR-550a-5p in 10 pairs of HCC tumor tissues (T) and paired paracancer normal tissues (N). F) Relative miR-550a-5p expression in 3 HCs compared with the normal hepatocyte cell line LO2. *p<0.05, **p<0.01, ***p<0.001

Decreased expression of miR-550a-5p can inhibit the proliferation and migration of HCs via the Wnt/β-catenin signaling pathway. To further explore the role of miR-550a-5p in the occurrence and development of HCC, we detected the expression levels of miR-550a-5p in three HCs by qPCR. The results showed that the expression levels of miR-550a-5p in the three HCs were all significantly increased compared with that in LO2 (Figure 1F). Among them, the top two highest expression levels were present in Huh7 and LM3 cells. Therefore, anti-miR-550a-5p was used to reduce the expression level of miR-550a-5p in these two HCs in subsequent experiments. The qPCR results showed that the expression of miR-550a-5p was significantly reduced in the HCs treated with anti-miR-550a-5p (Figure 2A). The results of the CCK-8 experiment showed that decreasing the expression of miR-550a-5p inhibited the proliferation of HCs (Figure 2B). Similarly, the EdU experiment results found that decreased miR-550a-5p could significantly reduce the number of HCs in the proliferative phase (Figure 2C). In the colony formation experiment, compared with the corresponding control group, the colonies number of the anti-miR-550a-5p group was significantly reduced (Figure 2D). In addition, the wound healing assays were performed to detect the effect of miR-550a-5p on the migration ability of Huh7 and LM3 cells, and the results illustrated that the wound distance was wider in the anti-miR-550a-5p group compared that in the control group, indicating that decreasing the expression of miR-550a-5p could inhibit the migration ability of HCs (Figure 2E). Similarly, the Transwell experiment results showed that decreased miR-550a-5p significantly reduced the number of Huh7 and LM3 cells in the chamber (Figure 2F). In addition, the WB results showed that after the miR-550a-5p expression was decreased, the marker related to cell proliferation ability (Ki-67) was significantly decreased. Meanwhile, the protein expression levels of N-cadherin and Vimentin were decreased, while the expression level of E-cadherin was increased, indicating that the migration ability of cells was weakened (Figures 3A, 3B). The activation of the Wnt/β-catenin signaling pathway was closely related to the proliferation and migration of HCC [19]. We found that decreasing the expression of miR-550a-5p could downregulate the protein expression levels of β-catenin and its downstream target proteins c-Myc, MMP2, and MMP9 (Figures 3C, 3D). Thus, our experiments showed that miR-550a-5p promoted the proliferation and migration of HCs partly via activating the Wnt/β-catenin signaling pathway.

Decreased expression of miR-550a-5p can inhibit HCC tumorigenicity in xenograft mice. To further explore the effect of miR-550a-5p on the growth of HCC *in vivo*, we established a mouse xenograft tumor model using Huh7 and LM3 cells. The tumor size and weight in the anti-miR-550a-5p group were significantly smaller than those in the control group (Figures 4A-4F). In addition, IHC staining was performed on tumor tissues and the results showed that knocking down the expression level of miR-550a-5p could reduce the positive rate of Ki-67 and cyclin B2 (CCNB2) (Figure 4G). Therefore, we concluded that decreasing the expression of miR-550a-5p could inhibit the tumorigenicity of HCC *in vivo*. Animal research was reviewed and approved by the Animal Ethics and Use Committee of the Second Clinical College of Chongqing Medical University.

miR-550a-5p directly interacted with GNE. To further explore the specific underlying mechanism of miR-550a-5p regarding promoting the progression of HCC, we used bioinformatics tools and combined TCGA database analysis to identify 11 downstream target genes of miR-550a-5p (Figure 5A). Among the five downregulated candidate genes, the function of GNE in HCC is unclear. Expression analysis of 50 pairs of HCC tissue samples in TCGA database showed that the expression level of GNE was significantly reduced in HCC (Figure 5B). In addition, patients with low expression of GNE had poor clinical outcomes (Figure 5C). Then, we found that there was a possible binding site between miR-550a-5p and the 3'-UTR of GNE mRNA on the Targets Scan online website (Figure 5D). And the luciferase reporter gene assay results showed that lower fluorescence activity was detected in the wild-type group compared to that in the mutant group in the case of simultaneous transfection of miR-550a-5p mimics, indicating that GNE was directly regulated by miR-550a-5p (Figure 5E). Moreover, RT-qPCR and WB were used to detect the mRNA and protein expression levels of GNE in tumor tissues and paired adjacent tissues of 10 HCC patients, and they were all reduced in tumor tissues (Figures 5F, 5G). In Huh7 and LM3 cells with low expression levels of miR-550a-5p, the mRNA and protein expression levels of GNE were significantly increased (Figures 5H, 5I). Therefore, miR-550a-5p might promote the occurrence of HCC by directly interacting with the tumor suppressor protein GNE.

GNE restored the suppressive effect of decreased miR-550a-5p. Next, rescue experiments were used to confirm that the oncogenic effect of miR-550a-5p was realized through the targeted inhibition of GNE. First, we interfered with the expression of GNE in Huh7 and LM3 cells with low expression levels of miR-550a-5p, and the mRNA and protein expression levels of GNE were significantly reduced (Figure 6A). Then, we used the above same cells to perform CCK-8, EdU, and colony formation experiments (Figures 6B–6D). The results showed that Huh7 and LM3 cells with low expression levels of miR-550a-5p and GNE had stronger proliferation ability than those with only low expression levels of miR-550a-5p. This suggested that the decreased expression of GNE could partly reverse the decreased proliferation capacity due to the decrease of miR-550a-5p. Similarly, we verified the impact of reduced GNE expression levels on the migration ability of HCC cells by wound healing and Transwell assays, and it was not unexpected to find that reduced GNE expression could also restore the weakened migration ability caused by decreased expression of miR-550a-5p (Figures 6E, 6F). In addition, the

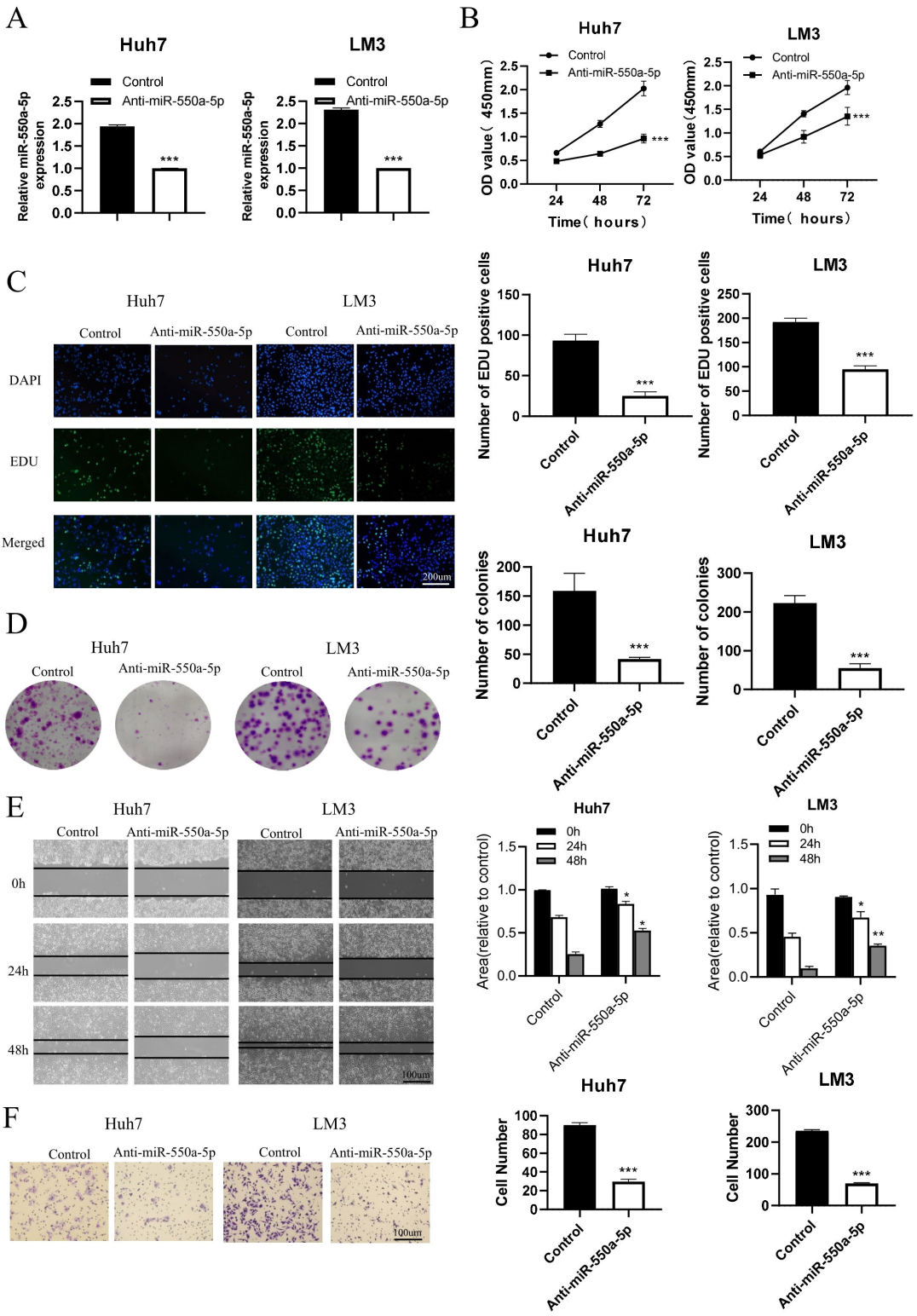

Figure 2. Decreased expression of miR-550a-5p inhibited the proliferation and migration of HCs. A) Quantitative real-time PCR (qRT-PCR) was used to measure miR-550a-5p expression in Huh7 and LM3 HCs transfected with miR-550a-5p inhibitor (anti-miR-550a-5p) or its associated control (control). Cell proliferation levels were analyzed in Huh7 and LM3 HCs transfected with anti-miR-550a-5p or control by cell-counting kit-8 (CCK-8) assay (B), 5-ethynyl-2'-deoxyuridine (EdU) assay (C) and colony-forming assay (D). Cell migration levels were analyzed in Huh7 and LM3 HCs transfected with anti-miR-550a-5p or control by wound healing assay (E) and Transwell assay (F). *p<0.05, **p<0.01, ***p<0.001

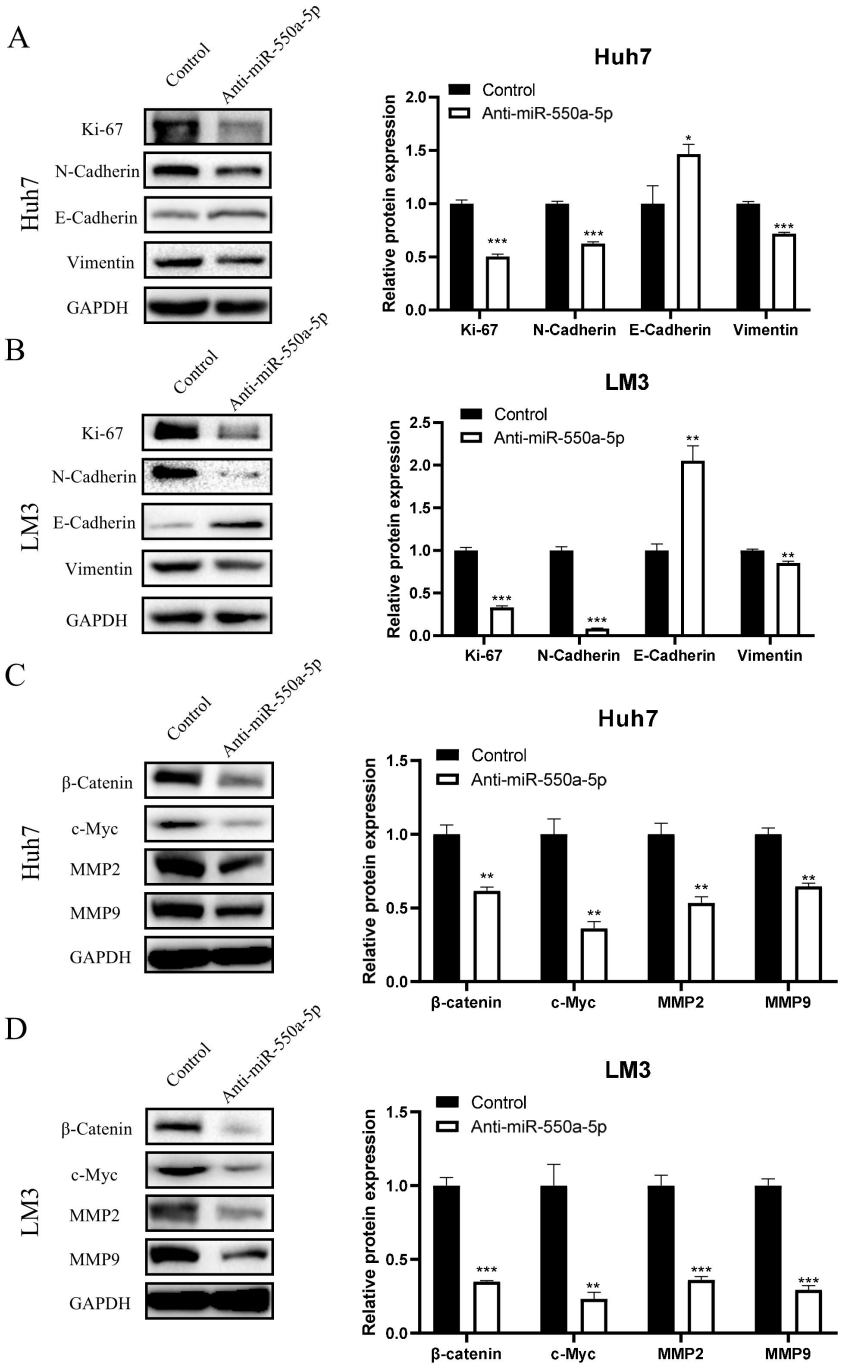

Figure 3. Decreased expression of miR-550a-5p inhibited the Wnt/β-catenin signaling pathway. A, B) The protein expression levels of proliferation- and migration-associated markers were measured by western blot in Huh7 and LM3 HCs transfected with miR-550a-5p inhibitor (anti-miR-550a-5p) or its associated control (control). C, D) The protein expression levels of the Wnt/β-catenin signaling pathway components were measured by western blot in Huh7 and LM3 HCs transfected with anti-miR-550a-5p or its associated control. *p<0.05, **p<0.01, ***p<0.001

WB results also showed that the siGNE group had stronger proliferation and migration ability than the NC group (Figures 7A, 7B). Decreased GNE elevated the expression level of β-catenin and its downstream molecules in Huh7 and LM3 cells transfected with the miR-550a-5p inhibitor (Figures 7C, 7D). Therefore, interference with GNE activated the Wnt/β-catenin signaling pathway and restored the inhibitory effect of reduced miR-550a-5p, further confirming that GNE was an important downstream target gene of miR-550a-5p.

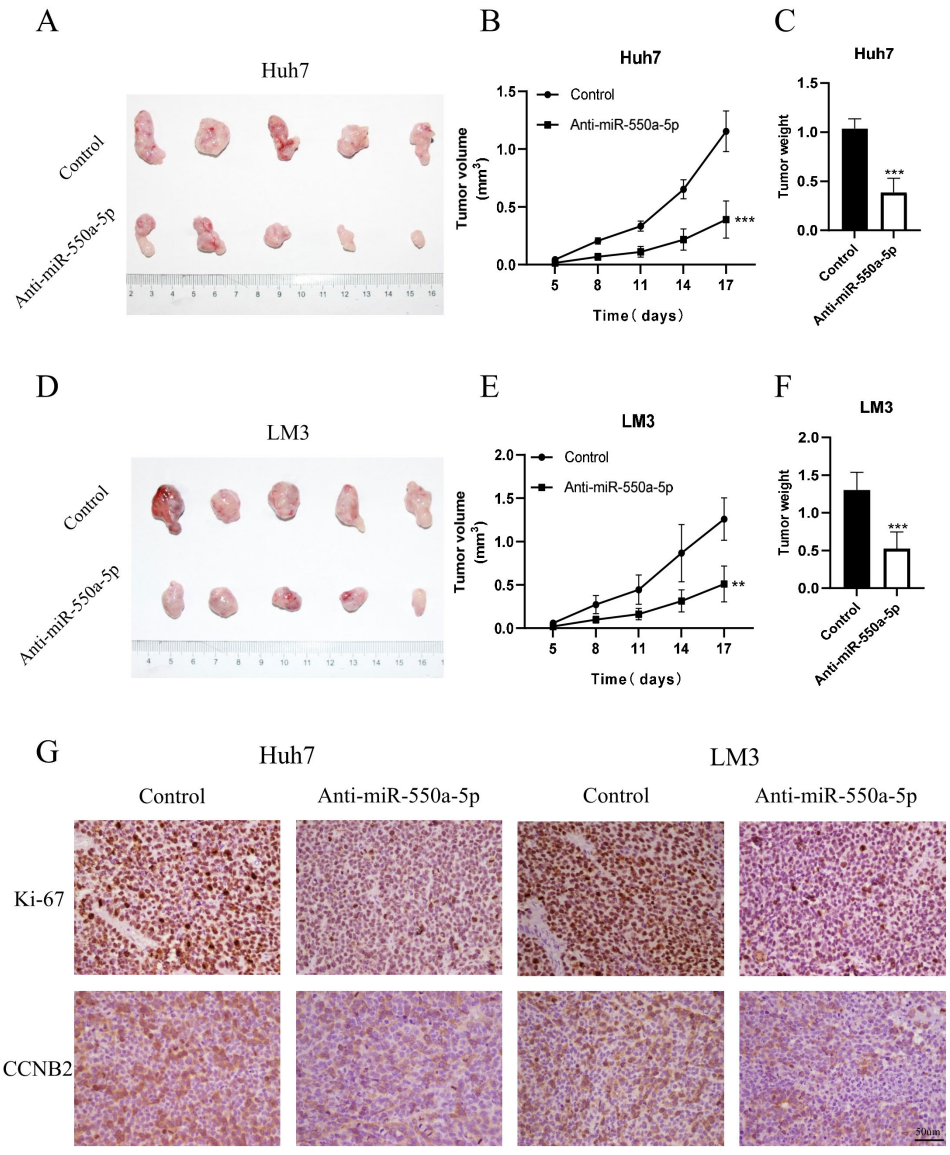

Figure 4. Decreased expression of miR-550a-5p inhibited the tumorigenicity of HCC *in vivo*. A) Huh7 and C) LM3 HCs transfected with miR-550a-5p inhibitor (anti-miR-550a-5p) or its associated control (control) were subcutaneously injected into nude mice for 17 days. B, D) Tumor volume was recorded every three days. C, E) Tumor weight was measured when the mice were sacrificed. F) The proliferation level of tumors was assessed by immunohistochemistry (IHC) staining. *p<0.05, **p<0.01, ***p<0.001

Discussion

Hepatocellular carcinoma (HCC) is one of the most common malignant tumors, and patients have a poor prognosis in the late stage [21]. However, the current tumor markers can only be detected in patients with advanced HCC, so it is urgent to find biomarkers for the early diagnosis of HCC. Although radiofrequency ablation, radiotherapy, transhepatic artery and portal vein chemotherapy, or transhepatic artery chemoembolization (TACE) have been widely used in the clinical treatment of unresectable HCC, the prognosis of HCC patients is still not optimistic. Many studies have demonstrated that miRNAs, as biomarkers, therapeutic targets, and prognostic indicators, play an important role in the diagnosis, treatment, and prognostic evaluation of HCC [22, 23]. In the current study, we found that miR-550a-5p can promote the proliferation and migration of HCC by directly binding to GNE via the Wnt/β-catenin signaling pathway (Figure 8).

In this study, we used TCGA database to analyze the differentially expressed miRNAs between tumor tissues and paired paracancer tissues of 48 HCC patients. We found

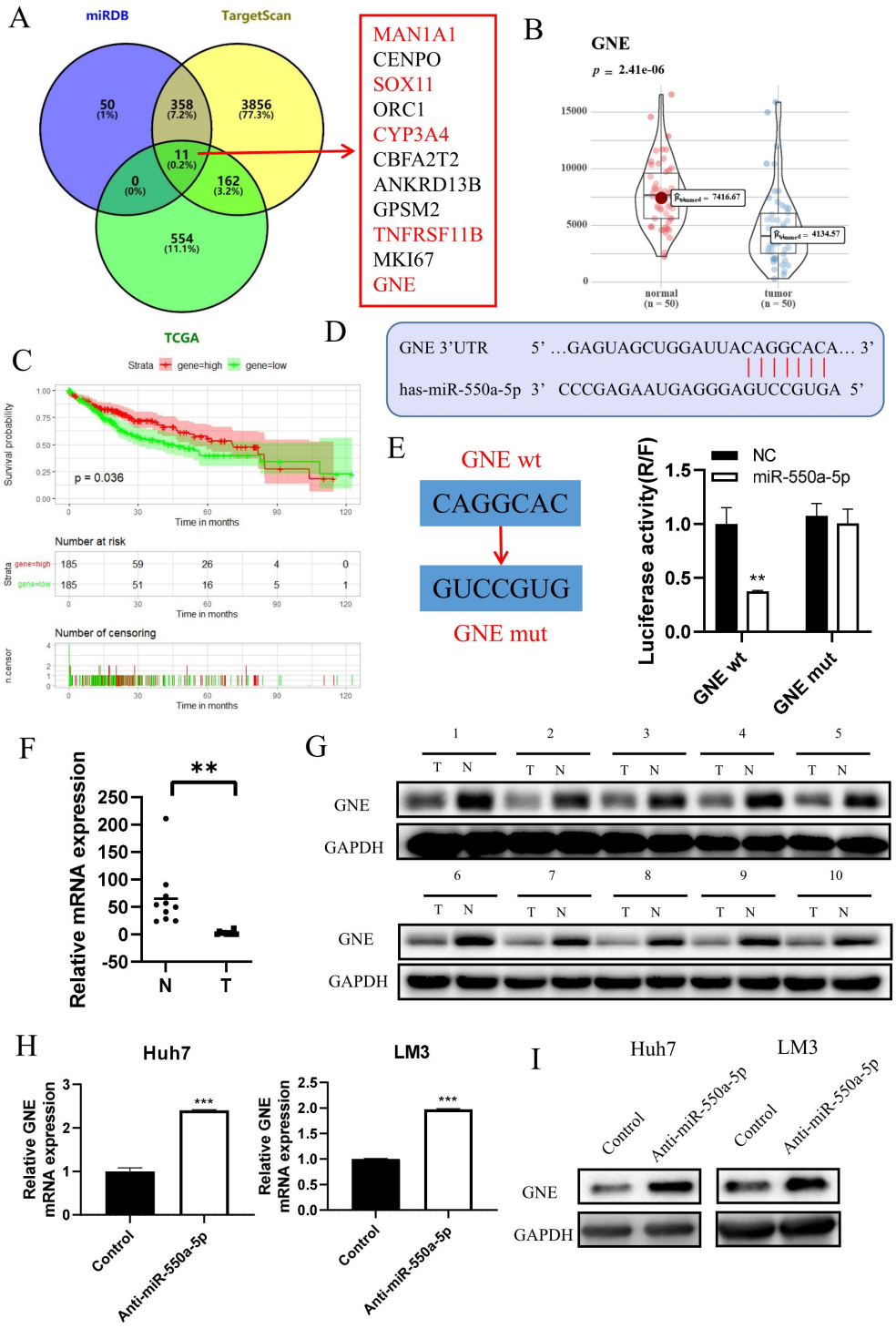

Figure 5. miR-550a-5p directly interacted with GNE and inhibited its expression. A) Venn diagram revealing potential target genes of miR-550a-5p by the miRDB, Target Scan, and TCGA databases. B) Relative mRNA expression of GNE in 50 pairs of HCC samples from TCGA database. C) Kaplan-Meier analysis of overall survival between high (n=185) and low (n=185) miR-550a-5p expression in HCC patients. D) Bioinformatics analysis of the possible binding site of miR-550a-5p and the GNE-3 '-UTR. E) A luciferase reporter gene assay was performed in LM3 HCs transfected with miR-550a-5p mimics (miR-550a-5p) or its negative control (NC) and WT-GNE-3'-UTR (GNE wt) or mut-GNE-3'-UTR (GNE mut) plasmids. F) Relative mRNA expression of GNE in 10 pairs of HCC tumor tissues (T) and paired paracancer normal tissues (N). G) Relative protein expression of GNE in 10 pairs of HCC tumor tissues (T) and paired paracancer normal tissues (N). H) The mRNA expression levels of GNE in Huh7 and LM3 HCs transfected with miR-550a-5p inhibitor (anti-miR-550a-5p) or its associated control (control). I) The protein expression levels of GNE in Huh7 and LM3 HCs transfected with anti-miR-550a-5p or control. *p<0.05, **p<0.01, ***p<0.001

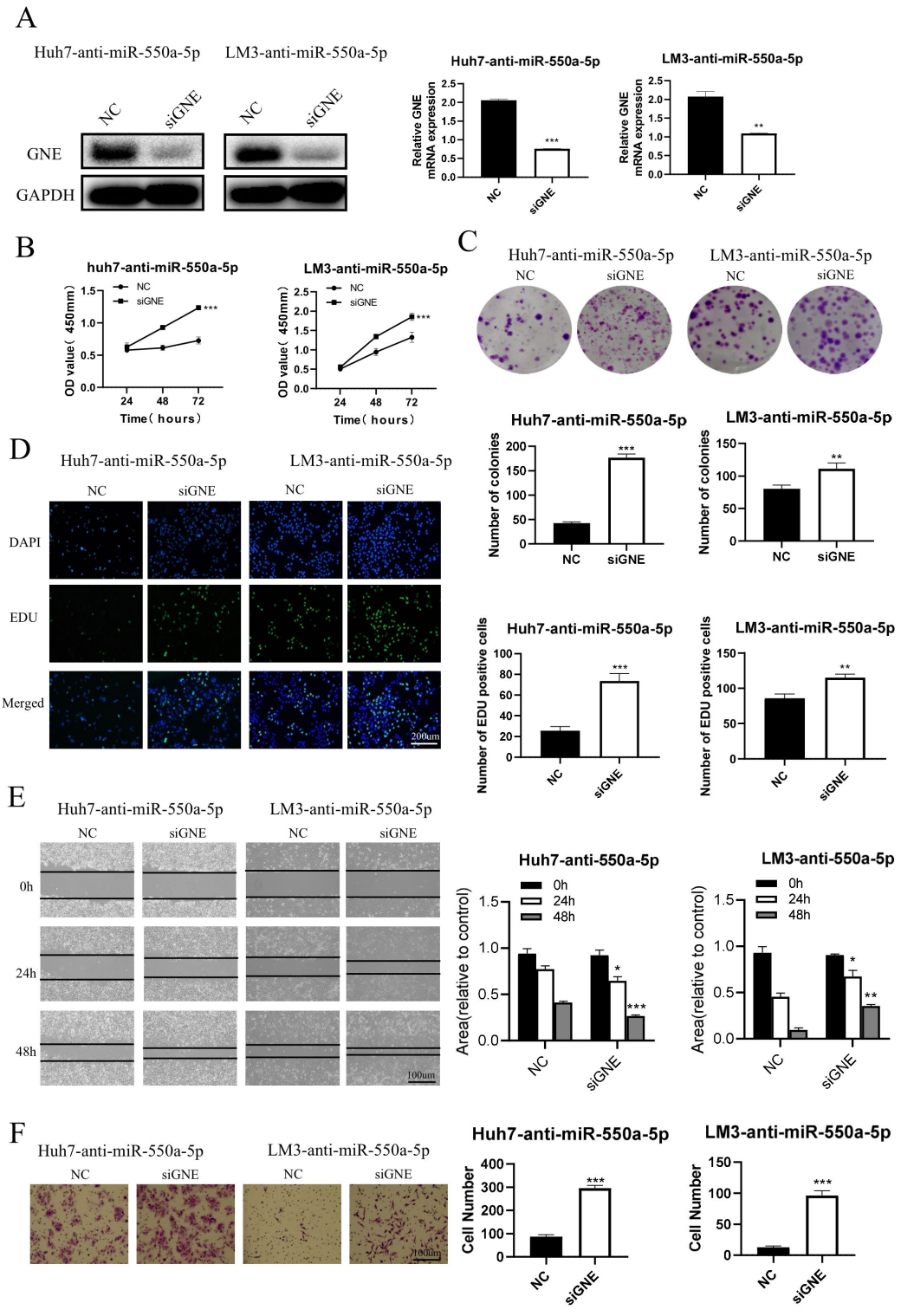

Figure 6. miR-550a-5p targeting of GNE promoted the proliferation and migration of HCs. A) Western blot (left panel) and quantitative real-time PCR (qRT–PCR) (right panel) were used to measure GNE protein and mRNA expression in Huh7 and LM3 HCs transfected with GNE small interfering RNA (siGNE) or negative control siRNA (NC) pretreated with miR-550a-5p inhibitor (anti-miR-550a-5p). The cell proliferation level was analyzed in Huh7-anti-miR-550a-5p and LM3-anti-miR-550a-5p HCs transfected with siGNE or NC by cell-counting kit-8 (CCK-8) assay (B), colony-forming assay (C) and 5-ethynyl-2'-deoxyuridine (EdU)assay (D). The cell migration level was analyzed in Huh7-anti-miR-550a-5p and LM3-anti-miR-550a-5p HCs transfected with siGNE or NC by wound healing assays (E) and Transwell assays (F). *p<0.05, **p<0.01, ***p<0.001

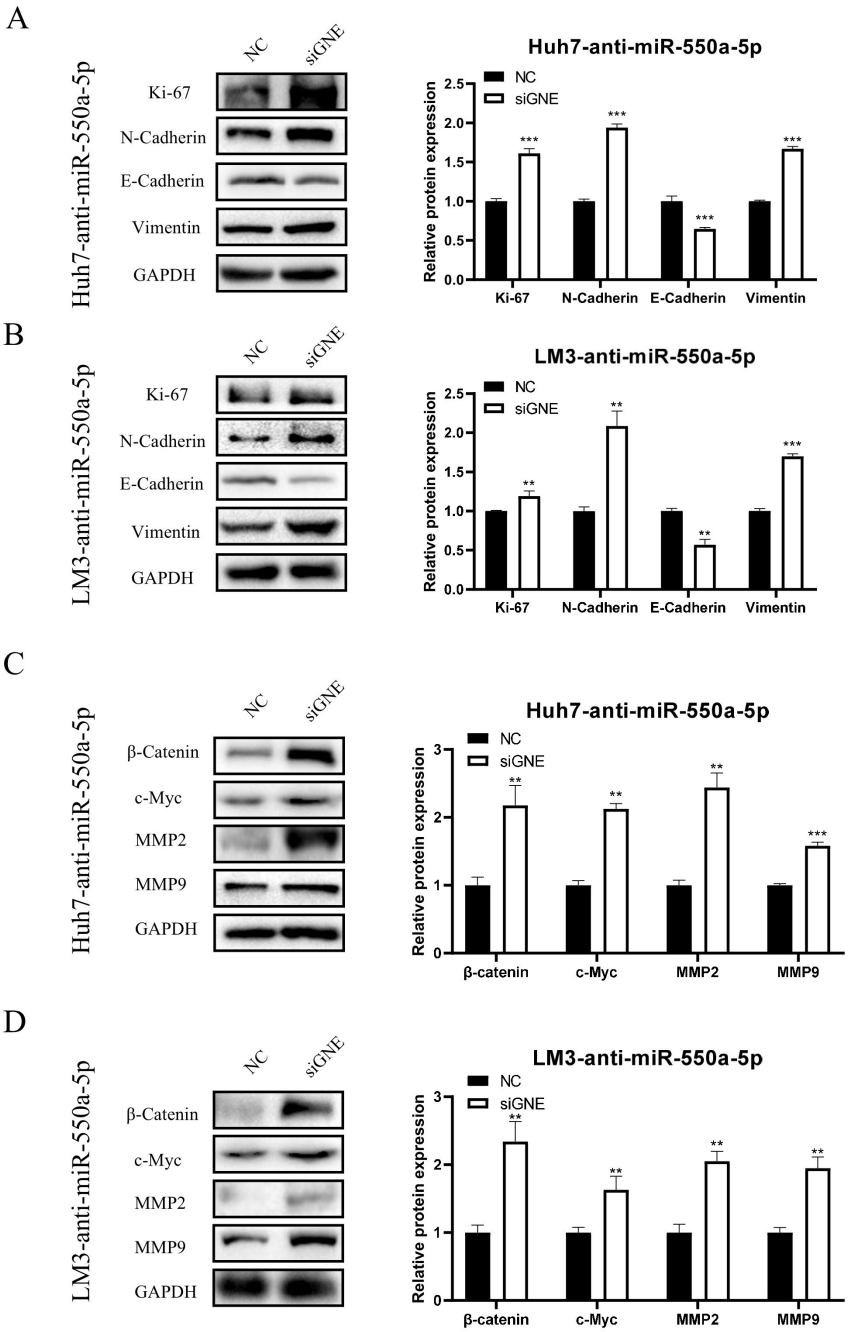

Figure 7. miR-550a-5p promoted the proliferation and migration of HCC by targeting GNE via the Wnt/β-catenin signaling pathway. A, B) The protein expression levels of proliferation- and migration-associated markers were measured by western blot in Huh7-anti-miR-550a-5p and LM3-anti-miR-550a-5p HCs transfected with GNE small interfering RNA (siGNE) or negative control siRNA (NC). C, D) The protein expression levels of the Wnt/β-catenin signaling pathway components were measured by western blot in Huh7-anti-miR-550a-5p and LM3-anti-miR-550a-5p HCs transfected with siGNE or NC. *p<0.05; **p<0.01; ***p<0.001

that miR-550a-5p expression was significantly upregulated in HCC tumor tissues and positively associated with the poor prognosis of HCC patients. The high expression of miR-550a-5p was subsequently validated in both HCC tissues and HCs. Wang et al. reported that miR-550a-5p can regulate colorectal cancer metastasis by targeting RNF43, an inhibitor of the Wnt/β-catenin signaling pathway [24]. Guo et al. identified miR-550a-5p as a tumor promoter by targeting LIMD1 in lung adenocarcinoma [25]. In a recent study, as a downstream target molecule of circCCDC85A, miR-550a-5p

promoted breast cancer progression by regulating MOB1A [26]. Circular RNA circCCDC85A inhibits breast cancer progression by acting as a miR-550a-5p sponge to enhance MOB1A expression. Our experiments verified that decreased expression of miR-550a-5p can inhibit the proliferation and migration of HCs and xenograft mice. In addition, we found that decreasing the expression of miR-550a-5p downregulated the protein expression levels of β-catenin and the downstream target proteins MMP2 and MMP9, which are biomarkers closely associated with HCC metastasis [27, 28].

Next, we demonstrated that miR-550a-5p directly interacts with GNE, a key enzyme in NeuAc biosynthesis [29]. GNE has been identified as a potential predictive biomarker for deoxynivalenol-induced liver damage [30]. However, the function of GNE in HCC is unclear. A luciferase reporter assay revealed that GNE is an important target gene of miR-550a-5p. Moreover, cell experiments demonstrated that GNE has a suppressor function in HCC. Decreased expression of GNE can increase the expression of the cell proliferation marker Ki-67 [31] and migration markers N-cadherin and Vimentin [32] in Huh7 and LM3 cells with reduced expression levels of miR-550a-5p. Therefore, a rescue experiment confirmed that GNE can restore the inhibitory effect of decreasing the expression of miR-550a-5p on the proliferation and migration of HCC.

Taken together, our study found that miR-550a-5p acts as a tumor promoter in HCC. In addition, we identified that miR-550a-5p directly targets GNE to affect the Wnt/β-catenin signaling pathway in HCs. We provided the first indication of the important role of miR-550a-5p in the development of HCC. Our findings break new ground for the early diagnosis, therapeutic drug development, and prognostic evaluation of HCC. Further research will focus on developing molecular targeted therapeutic drugs to prevent cancer progression, drug resistance, and distant metastasis.

Acknowledgments: We thank the Hepatobiliary Surgery Laboratory of Army Medical University for research equipment and technical support for this research.

References

[1] CHEN T. Circulating Non-Coding RNAs as Potential Diagnostic Biomarkers in Hepatocellular Carcinoma. J Hepatocell Carcinoma 2022; 9: 1029–1040. https://doi.org/10.2147/jhc.S380237

[2] NELSON ME, LAHIRI S, CHOW JD, BYRNE FL, HARGETT SR et al. Inhibition of hepatic lipogenesis enhances liver tumorigenesis by increasing antioxidant defence and promoting cell survival. Nat Commun 2017; 8: 14689. https://doi.org/10.1038/ncomms14689

[3] HOSSEINPOR S, KHALVATI B, SAFARI F, MIRZAEI A, HOSSEINI E. The association of plasma levels of miR-146a, miR-27a, miR-34a, and miR-149 with coronary artery disease. Mol Biol Rep 2022; 49: 3559–3567. https://doi.org/10.1007/s11033-022-07196-5

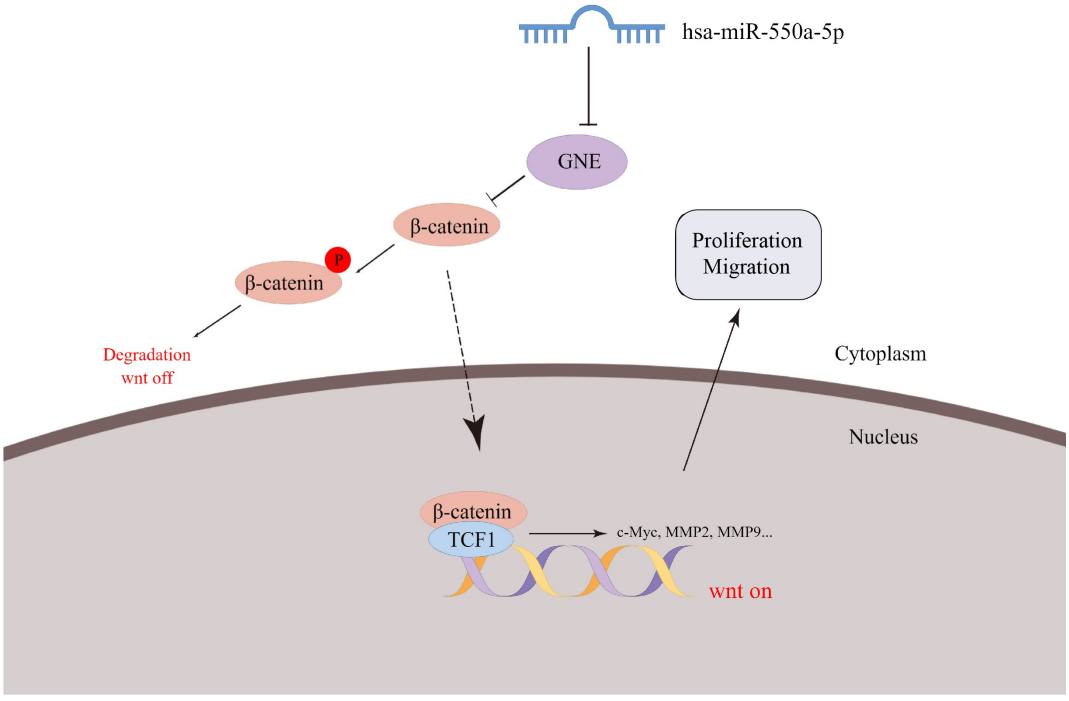

Figure 8. Graphical abstract of the role of miR-550a-5p in HCC. miR-550a-5p inhibits the expression of GNE, thereby promoting the proliferation and migration of HCC via the Wnt/β-catenin signaling pathway.

[4] BRONTE F, BRONTE G, FANALE D, CARUSO S, BRONTE E et al. HepatomiRNoma: The proposal of a new network of targets for diagnosis, prognosis and therapy in hepatocellular carcinoma. Crit Rev Oncol Hematol 2016; 97: 312–321. https://doi.org/10.1016/j.critrevonc.2015.09.007

[5] WANG XW, HEEGAARD NH, ORUM H. MicroRNAs in liver disease. Gastroenterology 2012; 142: 1431–1443. https://doi.org/10.1053/j.gastro.2012.04.007

[6] DU J, JIA F, WANG L. Advances in the Study of circRNAs in Hematological Malignancies. Front Oncol 2022; 12: 900374. https://doi.org/10.3389/fonc.2022.900374

[7] SI W, SHEN J, ZHENG H, FAN W. The role and mechanisms of action of microRNAs in cancer drug resistance. Clin Epigenetics 2019; 11: 25. https://doi.org/10.1186/s13148-018-0587-8

[8] LIU Y, WANG J, CHEN J, WU S, ZENG X et al. Upregulation of miR-520c-3p via hepatitis B virus drives hepatocellular migration and invasion by the PTEN/AKT/NF-κB axis. Mol Ther Nucleic Acids 2022; 29: 47–63. https://doi.org/10.1016/j.omtn.2022.05.031

[9] WANG L, LI B, BO X, YI X, XIAO X et al. Hypoxia-induced LncRNA DACT3-AS1 upregulates PKM2 to promote metastasis in hepatocellular carcinoma through the HDAC2/FOXA3 pathway. Exp Mol Med 2022; 54: 848–860. https://doi.org/10.1038/s12276-022-00767-3

[10] REINKE SO, LEHMER G, HINDERLICH S, REUTTER W. Regulation and pathophysiological implications of UDP-GlcNAc 2-epimerase/ManNAc kinase (GNE) as the key enzyme of sialic acid biosynthesis. Biol Chem 2009; 390: 591–599. https://doi.org/10.1515/bc.2009.073

[11] ISHTIAQ H, SIDDIQUI S, NAWAZ R, JAMALI KS, KHAN AG. Sialuria-Related Intellectual Disability in Children and Adolescent of Pakistan: Tenth Patient Described has a Novel Mutation in the GNE Gene. CNS Neurol Disord Drug Targets 2020; 19: 127–141. https://doi.org/10.2174/1871527319666200213115747

[12] TORCHIA E, LUCCHINI M, BORTOLANI S, MONFORTE M, GARIBALDI M et al. Upper body involvement in GNE myopathy assessed by muscle imaging. Neuromuscul Disord 2022; 32: 410–418. https://doi.org/10.1016/j.nmd.2021.12.007

[13] PARK JC, KIM J, JANG HK, LEE SY, KIM KT et al. Multiple isogenic GNE-myopathy modeling with mutation specific phenotypes from human pluripotent stem cells by base editors. Biomaterials 2022; 282: 121419. https://doi.org/10.1016/j.biomaterials.2022.121419

[14] SUN H, ZHOU Y, JIANG H, XU Y. Elucidation of Functional Roles of Sialic Acids in Cancer Migration. Front Oncol 2020; 10: 401. https://doi.org/10.3389/fonc.2020.00401

[15] BASSAGAÑAS S, PÉREZ-GARAY M, PERACAULA R. Cell surface sialic acid modulates extracellular matrix adhesion and migration in pancreatic adenocarcinoma cells. Pancreas 2014; 43: 109–117. https://doi.org/10.1097/MPA.0b013e31829d9090

[16] HE J, ZHAO H, DENG D, WANG Y, ZHANG X et al. Screening of significant biomarkers related with prognosis of liver cancer by lncRNA-associated ceRNAs analysis. J Cell Physiol 2020; 235: 2464–2477. https://doi.org/10.1002/jcp.29151

[17] XUE C, LI G, ZHENG Q, GU X, BAO Z et al. The functional roles of the circRNA/Wnt axis in cancer. Mol Cancer 2022; 21: 108. https://doi.org/10.1186/s12943-022-01582-0

[18] SELVAGGI F, CATALANO T, COTELLESE R, ACETO GM. Targeting Wnt/β-Catenin Pathways in Primary Liver Tumours: From Microenvironment Signaling to Therapeutic Agents. Cancers (Basel) 2022; 14: 1912. https://doi.org/10.3390/cancers14081912

[19] XU Y, YU X, SUN Z, HE Y, GUO W. Roles of lncRNAs Mediating Wnt/β-Catenin Signaling in HCC. Front Oncol 2022; 12: 831366. https://doi.org/10.3389/fonc.2022.831366

[20] XIE J, CHEN L, SUN Q, LI H, WEI W et al. An immune subtype-related prognostic signature of hepatocellular carcinoma based on single-cell sequencing analysis. Aging (Albany NY) 2022; 14: 3276–3292. https://doi.org/10.18632/aging.204012

[21] HAN Z, FENG W, HU R, GE Q, MA W et al. RNA-seq profiling reveals PBMC RNA as a potential biomarker for hepatocellular carcinoma. Sci Rep 2021; 11: 17797. https://doi.org/10.1038/s41598-021-96952-x

[22] KHASHKHASHI MOGHADAM S, BAKHSHINEJAD B, KHALAFIZADEH A, MAHMUD HUSSEN B, BABASHAH S. Non-coding RNA-associated competitive endogenous RNA regulatory networks: Novel diagnostic and therapeutic opportunities for hepatocellular carcinoma. J Cell Mol Med 2022; 26: 287–305. https://doi.org/10.1111/jcmm.17126

[23] ZHANG Y, SHAO J, LI S, LIU Y, ZHENG M. The Crosstalk Between Regulatory Non-Coding RNAs and Nuclear Factor Kappa B in Hepatocellular Carcinoma. Front Oncol 2021; 11: 775250. https://doi.org/10.3389/fonc.2021.775250

[24] WANG G, FU Y, YANG X, LUO X, WANG J et al. Brg-1 targeting of novel miR550a-5p/RNF43/Wnt signaling axis regulates colorectal cancer metastasis. Oncogene 2016; 35: 651–661. https://doi.org/10.1038/onc.2015.124

[25] GUO ZZ, MA ZJ, HE YZ, JIANG W, XIA Y et al. miR-550a-5p Functions as a Tumor Promoter by Targeting LIMD1 in Lung Adenocarcinoma. Front Oncol 2020; 10: 570733. https://doi.org/10.3389/fonc.2020.570733

[26] MENG L, CHANG S, SANG Y, DING P, WANG L et al. Circular RNA circCCDC85A inhibits breast cancer progression via acting as a miR-550a-5p sponge to enhance MOB1A expression. Breast Cancer Res 2022; 24: 1. https://doi.org/10.1186/s13058-021-01497-6

[27] DU D, LIU C, QIN M, ZHANG X, XI T et al. Metabolic dysregulation and emerging therapeutical targets for hepatocellular carcinoma. Acta Pharm Sin B 2022; 12: 558–580. https://doi.org/10.1016/j.apsb.2021.09.019

[28] HASSAN HM, EL-KANNISHY SMH, ALATTAR A, ALSHAMAN R, HAMDAN AM et al. Therapeutic effects of blocking β-catenin against hepatocellular carcinoma-induced activation of inflammation, fibrosis and tumor invasion. Biomed Pharmacother 2021; 135: 111216. https://doi.org/10.1016/j.biopha.2021.111216

[29] YONEKAWA T, MALICDAN MC, CHO A, HAYASHI YK, NONAKA I et al. Sialyllactose ameliorates myopathic phenotypes in symptomatic GNE myopathy model mice. Brain 2014; 137: 2670–2679. https://doi.org/10.1093/brain/awu210

[30] LIAO Y, PENG Z, WANG L, LI D, YUE J et al. Long noncoding RNA Gm20319, acting as competing endogenous RNA, regulated GNE expression by sponging miR-7240-5p to involve in deoxynivalenol-induced liver damage in vitro. Food Chem Toxicol 2020; 141: 111435. https://doi.org/10.1016/j.fct.2020.111435

[31] QIN LX, TANG ZY. The prognostic molecular markers in hepatocellular carcinoma. World J Gastroenterol 2002; 8: 385–392. https://doi.org/10.3748/wjg.v8.i3.385

[32] LIU T, LIAO S, MO J, BAI X, LI Y et al. LncRNA n339260 functions in hepatocellular carcinoma progression via regulation of miRNA30e-5p/TP53INP1 expression. J Gastroenterol 2022; 57: 784–797. https://doi.org/10.1007/s00535-022-01901-8